Electronic Supplementary Information

Cite this: DOI: 10.1039/x0xx00000x

Solvent-Free Synthesis of an Ionic Liquid Integrated Ether-Abundant Polymer as a Solid Electrolyte for Flexible Electric Double-Layer Capacitors

Ruiqi Na,[a,b] Ching-Wen Su,[b] Yi-Han Su,[b] Yu-Chun Chen,[b] Yen-Ming Chen,[b] Guibin Wang*[a] and Hsisheng Teng*[b]

[a]College of Chemistry, Key Laboratory of High Performance Plastics, Ministry of Education, Jilin University, Changchun, 130012, P. R. China. E-mail: wgb@jlu.edu.cn; Fax: +0086-431-85168889; Tel: +0086-431-85168889

[b]Department of Chemical Engineering and Research Center for Energy Technology and Strategy, National Cheng Kung University, Tainan, 70101, Taiwan. E-mail: hteng@mail.ncku.edu.tw; Fax: +886-6-2344496; Tel: +886-6-2385371

Electronic supplementary information for:

1. The reaction mechanism of polymerization to form cross-linked (PEO-A) network structure.

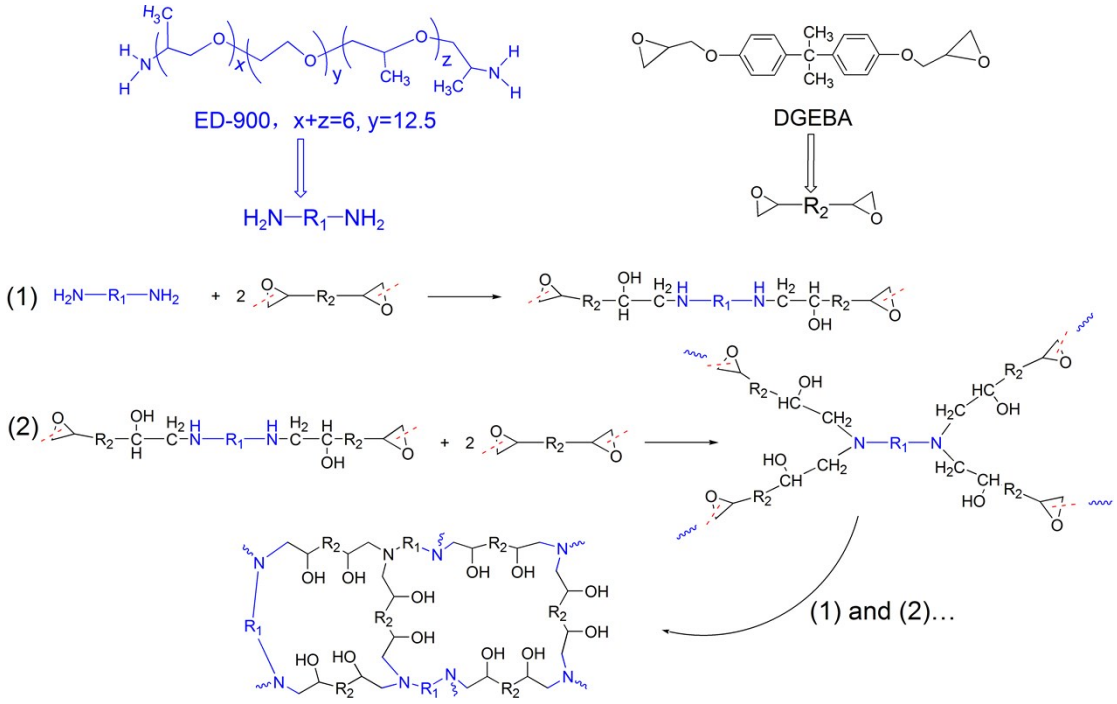

Scheme S1. The reaction mechanisms of polymerization between the epoxy and amine groups to form (PEO-A) epoxy-resin network structure.

2. FTIR spectra of DGEBA, ED-900 and (PEO-A) polymer.

Herein, FTIR was carried out to characterize the chemical structure of synthesized cross-linked (PEO-A) polymer. The FTIR spectra of DGEBA, ED-900 monomer and (PEO-A) polymer are shown in Fig. S1. For ED-900, the peaks at 2876 cm^{-1} and 1460, 1360 cm^{-1} are ascribed to the stretching vibration of alkyl groups and bending signals of $-CH_2-$ and $-CH_3$, respectively, and the peak at 1098 cm^{-1} corresponding to the C-O-C stretching. The peaks at 1610 and 1510 cm^{-1} are ascribed to the aromatic C-C stretching of benzene rings of DGEBA. These signals are also be found in cross-linked (PEO-A) polymer spectrum. However, compared with the FTIR spectra of DGEBA, The 900 cm^{-1} peak for epoxy stretching did not appear in the cross-linked (PEO-A) polymer spectrum, whereas the 930 cm^{-1} peak for C-N bonding was present. Meanwhile, the $-NH_2$ peak of ED-900 also disappeared in the cross-linked (PEO-A) polymer system. This FTIR results suggest that the bridging reactions occurred between the amine groups of ED-900 and the epoxy groups of DGEBA, and the cross-linked framework was formed.

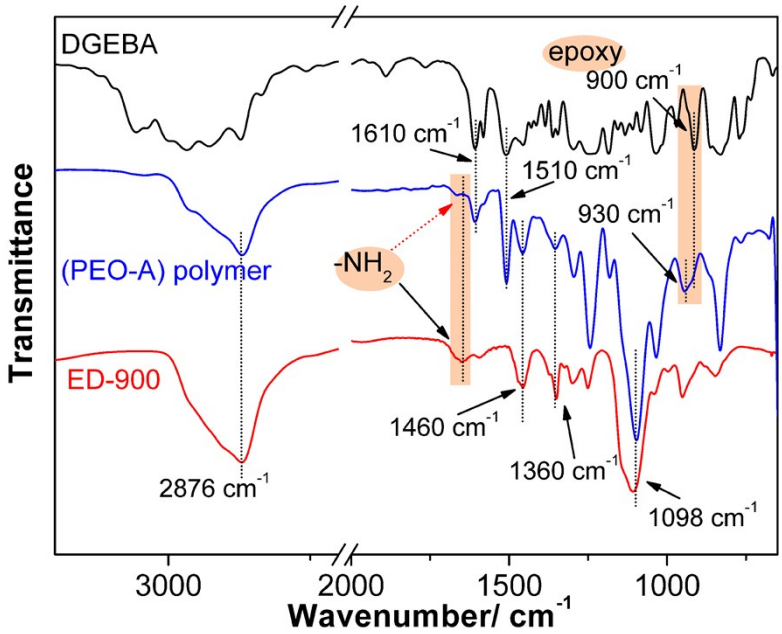

Fig. S1 FTIR spectra of DGEBA, ED-900 monomer and cross-linked (PEO-A) polymer.

3. Impedance spectra of the electrolytes for conductivity calculation

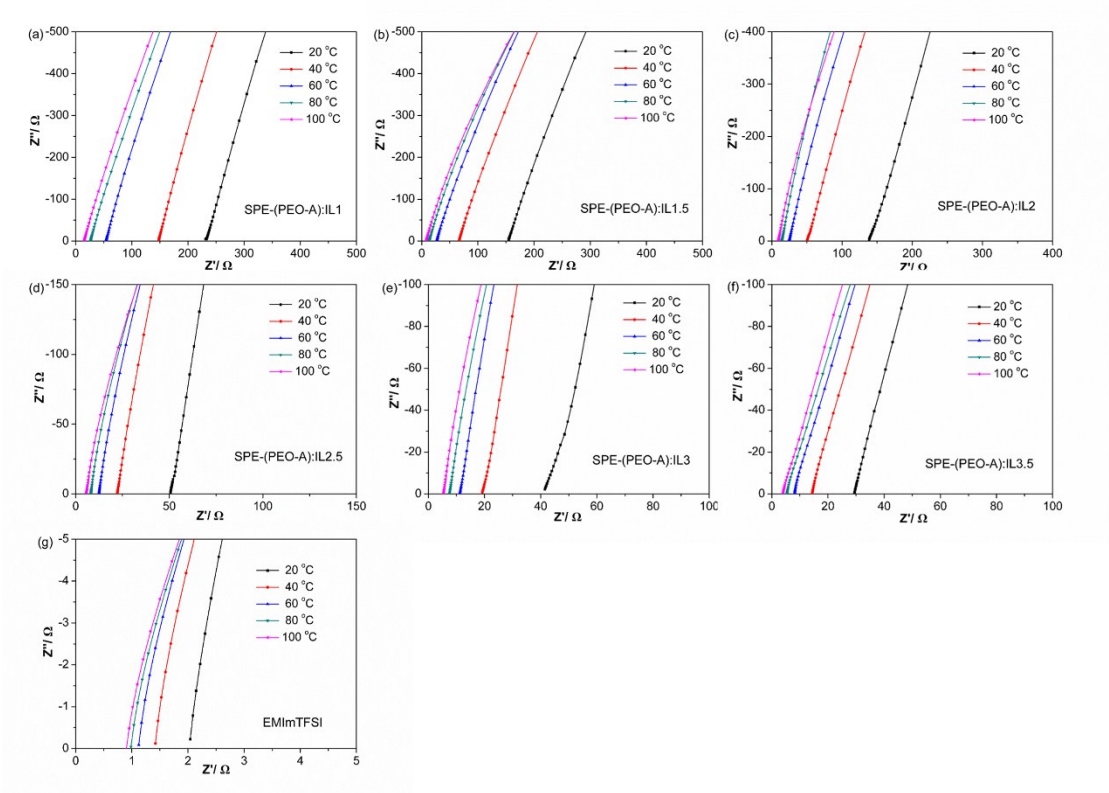

Fig. S2 Nyquist impedance spectra of electrolytes at various temperatures: (a) SPE-(PEO-A):IL1, 310 μm; (b) SPE-(PEO-A):IL1.5, 300 μm; (c) SPE-(PEO-A):IL2, 470 μm; (d) SPE-(PEO-A):IL2.5, 430 μm; (e) SPE-(PEO-A):IL3, 450 μm; (f) SPE-(PEO-A):IL3.5, 360 μm; (g) EMImTFSI, 40 μm. The measurements were conducted by inserting the electrolytes between two stainless-steel electrodes and applying an AC potential amplitude of 5 mV over a frequency range of 1 to 100k Hz at temperatures of 20 to 100 °C. The thicknesses of the electrolytes are provided following the electrolyte codes. The impedance spectra of EMImTFSI were measured using a cellulose membrane as the support.

4. Photographs of SPE-(PEO-A):IL3 and SPE-(PEO-A):IL3.5.

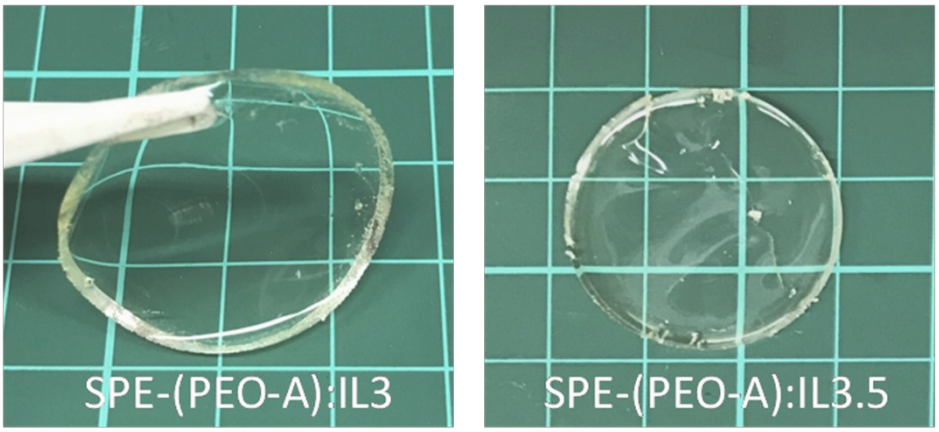

Fig. S3 The photographs of SPE-(PEO-A):IL3 and SPE-(PEO-A):IL3.5. When peeled from the PP plate, the SPE-(PEO-A):IL3.5 film was broken because it was too soft and fragile to maintain the mechanical strength.

5. Cross sectional SEM image of EDLC-SPE-(PEO-A):IL.

The cross-sectional SEM image of the EDLC-SPE-(PEO-A):IL at different magnifications is given in Fig. S3(a) and (b). It can be seen that the AC electrode and SPE-(PEO-A):IL electrolyte were integrated into a concrete in the EDLC device and no delamination was observed. This experimental evidence supports the claim that the SPE-(PEO-A):IL is directly synthesized on the carbon electrodes and provides a better electrode–electrolyte interface.

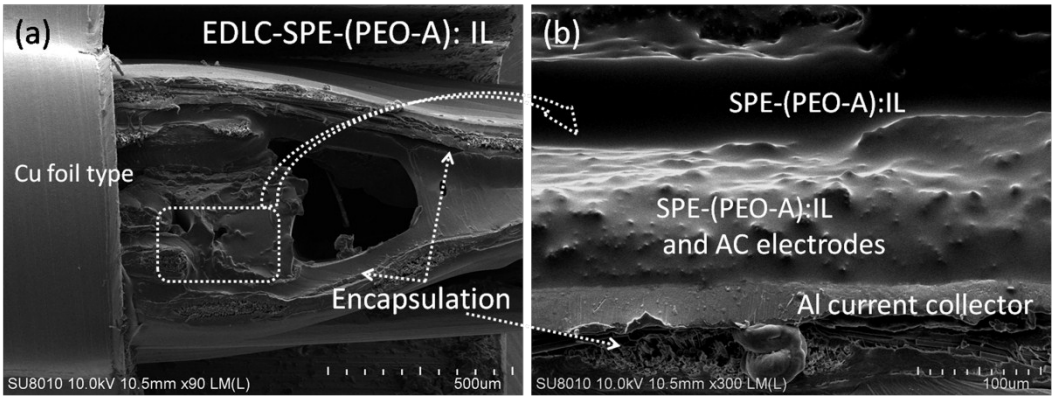

Fig. S4 The cross sectional SEM images of the EDLC-SPE-(PEO-A):IL at different magnifications with (a) size of 500 μm and (b)size of 100 μm.

6. Cyclic voltammograms of the EDLC-EMImTFSI and EDLC-SPE-(PEO-A):IL measured at 10–200 mV s^{-1}.

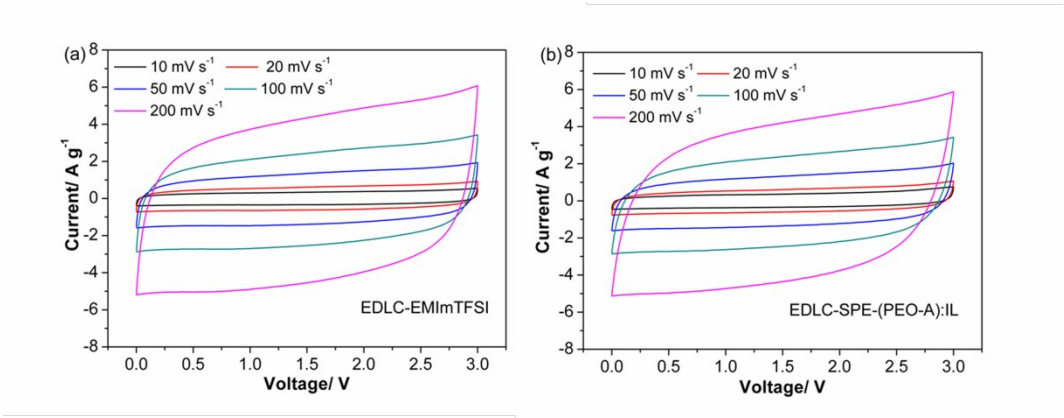

Fig. S5 Cyclic voltammograms of (a) EDLC-EMImTFSI and (b) EDLC-SPE-(PEO-A):IL at various scan rates of 10–200 mV s^{-1}.

7. Galvanostatic charge-discharge curves of the EDLC-EMImTFSI and EDLC-SPE-(PEO-A):IL measured at 0.5–10 A g^{-1}.

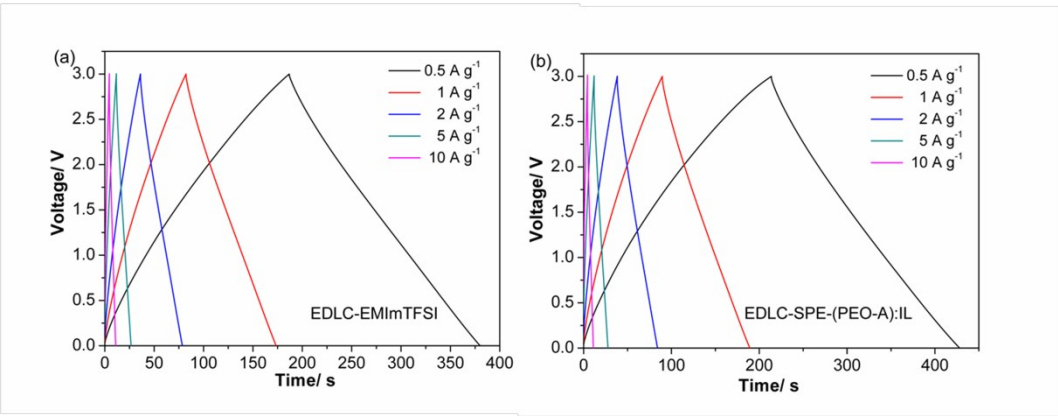

Fig. S6 The voltage-time curves of (a) EDLC-EMImTFSI and (b) EDLC-SPE-(PEO-A):IL charged-discharged at various discharge rates of 0.5−10 A g^{-1}.

8. Galvanostatic charge-discharge curves of EDLC-SPE-(PEO-A):IL after different times of cycling.

The stability of the EDLC-SPE-(PEO-A):IL has also been tested by recording the voltage–time curves after different times of cycling (Fig. S6). Almost no deviation in the shape of the voltage-time curves has been observed for different cycles, which further confirms the stability of the EDLC device.

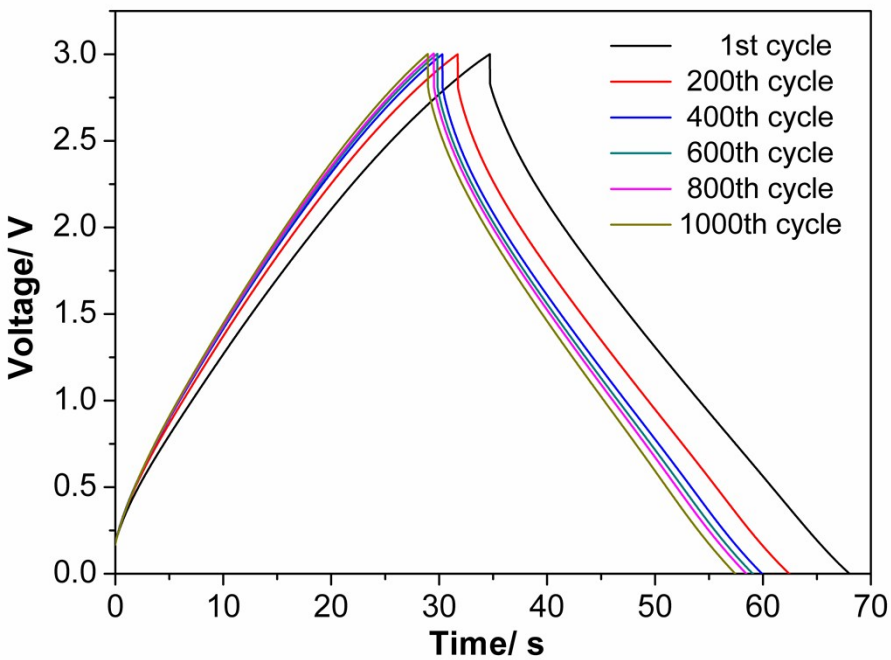

Fig. S7 The voltage–time curves of EDLC-SPE-(PEO-A):IL after different times of cycling.

9. Detailed electrochemical performance data of EDLC-EMImTFSI and EDLC-SPE-(PEO-A):IL.

Table S1. Specific capacitances, energy densities and power densities of EDLC-EMImTFSI and EDLC-SPE-(PEO-A):IL at different current densities.

Current density ($A\ g^{-1}$)	EDLC-EMImTFSI			EDLC-SPE-(PEO-A):IL		
	C_s[a]	E_{cell}[a]	P_{cell}[a]	C_s	E_{cell}	P_{cell}
0.5	129.7	40.2	746.6	133.9	41.2	692.6
1	123.3	37.9	1488.5	125.6	38.3	1377.7
2	115.3	35.0	2956.1	114.4	34.1	2724.4
3	106.4	32.9	4401.0	108.3	31.5	4038.5
5	103.2	29.9	7226.5	99.3	27.5	6574.6
10	92.3	24.8	13906.5	86.8	21.1	12314.6

[a] C_s, E_{cell} and P_{cell} were specific capacitances ($F\ g^{-1}$), energy densities ($Wh\ kg^{-1}$) and power densities ($W\ kg^{-1}$), respectively, and all obtained from GCD measurements at different current densities.

10. Low-temperature electrochemical performance of EDLC-EMImTFSI and EDLC-SPE-(PEO-A):IL

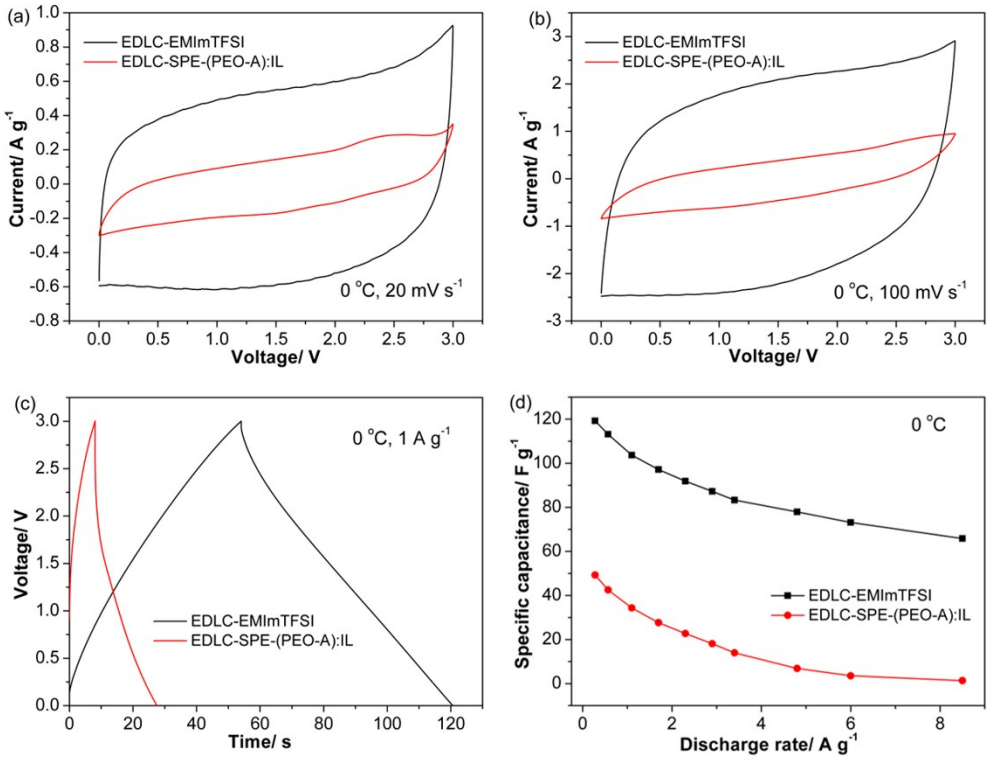

Fig. S8 Electrochemical performance of the EDLC-EMImTFSI and EDLC-SPE-(PEO-A):IL at 0 °C: (a and b) Cyclic voltammograms measured at 10 and 100 mV s^{-1}; (c) typical voltage–time curves of charge and discharge at 1 A g^{-1}; (d) variation of the specific capacitance value with the discharge rate.